REMARKS ON THE R- CURVE BEHAVIOR OF CERAMICS

F. E. Buresch[1]

Two types of residual stresses are proposed to be responsible for failure of ceramics. Residual stresses of the 2. kind act in the phase and grain boundaries, due to thermal mismatch and induce microcracking. Residual stresses of the 1. kind originate from elastic mismatch on the boundary of the damage zone, and are due to local stress redistribution during the quantized crack growth. The latter induces an internal bending moment which keeps the crack open at zero load. The processes which involve both kinds of residual stresses during loading of a body, can enhance the fracture toughness of specific ceramics.

INTRODUCTION

Failure of ceramics is preceded by stress induces microcracking as a consequence of the superposition of an external load with a residual stress field, which is due to a thermomechanical mismatch between grains and phase (1). This is well documented by photoelastic coatings (2), a special decoration technique for the visualization of microcracks and similar defects based on chemical impregnation and transmitted light optical investigation (3), acoustic emission analysis (AE) (4) and with small angle X ray scattering (SAXS) (5).

The residual stress induced micromechanical strain energy release rate $\tilde{G}_r$, linearly increases with the grain facet size 2a (6). As shown with AE during monotonic loading of a ceramic, microcracking starts at lower load in a coarse and then in a fine grained ceramic. In addition, as shown experimentally with coarse grained ceramics, the beginning of microcracking can be identified with the elastic limit P. With increasing load, a microcracked process zone develops ahead of a critical crack or notch. At a critical strain energy density inside the process zone, favorable orientated microcracks are either joined with, or to a macrocrack. After some stress redistribution, a new process zone will be build up. Thus, during monotoning straining of a body, the crack jumps in discrete steps, if the critical state of the damage zone is given. This process

[1]Institute for Computer Application, University of Stuttgart, FRG.

includes local alternating unloading and reloading of the frontal damage zone. It was analytically shown that these mechanisms produce residual stresses of the 1. kind on the border of the damage zone (1). However, with photoelastic coatings it was experimentally shown that, during an incremental crack growth, the surface of the damage zone is free of normal stresses (2). Thus, the residual stresses of the first kind generate in the interior of the fracture zone of the wake radial compression, and on its surface tangential tension stresses, which was verified by X–ray fractography (7).

The purpose of this work was, to demonstrate the dominating influence of the state of the residual stresses of the elastic damage zone on the $\tilde{G}_R$ curve behavior of brittle materials.

THE STATE OF THE ELASTIC DAMAGE ZONE

The structure of the microcrack field in the damage zone of a macrocrack strongly depends on its velocity. This was demonstrated for a glass ceramic, and also holds for alumina (5,8). With decreasing velocity, the size of the elastic damage zone, and the density of microcracks increases. Also, the orientation of the microcracks, with respect to the macrocrack, became more irregular. Fig. 1 shows a macrocrack which was induced by rapid cooling of a body of relatively coarse grained alumina (9). A macrocrack surrounds a damage zone with a depth of up to 10 times the average grain size. In this case, the orientation of the microcracks, with respect to the macrocrack, is very diffuse. It seems that the portion of "mode II" microcracks is high. Optical analysis with the Quantimet 570 (Leitz Co.) of the elastic damage zone of the crack of the relatively coarse grained alumina AF 997, demonstrate a predominantly parallel orientation of more than ten percent of the microcracks, with respect to the macrocrack. This follows also from SAXS measurements (5). In the case of this material, the size of the damage zone varies from about ten times of the average grain sizes at low crack velocities, down to about 3 times at high crack velocities.

However, it was analytically shown (10) that, in addition to the size of the damage zone and the density of microcracks, their orientation has an important influence on the crack resistance due to elastic interaction effects (10), with respect to the macrocrack. This also holds true for the absolute value of the reduced Young's modulus. For example, in previous papers it was analytically shown, that within the diamond-like crack system, the Young's modulus is not unique at a specific crack density. With densities of parallel and colinear oriented cracks of 60% and 50% respectively, the reduction yields 35%. However, with an equal total crack density of 30% within the same crack systems, the reduction reduces to only 20% if the densities of parallel and colinear oriented cracks are 50% and 60%, respectively. The effect is due to differences in the elastic interaction between the two crack orientations. In the first case, all crack tips are oriented one upon the other, which yields a high stress concentration.

The influence of the different crack configurations is much more pronounced, with respect to I_m (eq. 7) as shown in (10). In the first case, the normalized crack resistance yields 0.75, whereas in the second case the value is 1.05. Thus, the elastic interaction effect on the crack resistance changes from strong anti-shielding to crack tip shielding.

If the density of active microcrack nuclei is reduced due to thermal shock (5) or spontaneous microcracking as a consequence of a phase transformation (11), the effective reduction of Young's modulus $\Delta E = E - E_m$, and also the crack resistance decreases. These processes are inherent in the development of the residual stresses of the damage zone, which will be reviewed in the following.

THE EFFECTIVE CRACK RESISTANCE OF CERAMICS

The essential features of a load displacement (P–u) diagram are the evaluation of the total displacement u_a as the sum of the local elastic, and the residual displacement during crack growth given as

$$u_a = u_e + u_r \tag{1}$$

This is equivalent to the following compliance equation

$$C_a = C_e + C_r \tag{2}$$

The same formalism holds for the parameters of crack resistance in the following

$$\tilde{G}_R = \tilde{G}_e + \tilde{G}_r \tag{3}$$

which is given with measured values of P, C_e, u_r and the actual crack length a as (12,13)

$$\tilde{G}_R = \frac{P^2}{2}\,\frac{d}{da}(2C_a - C_e) + P(2C_a - C_e)\frac{dP}{da} \tag{4}$$

The $\tilde{G}_R$ curve of brittle materials has a maximum $\tilde{G}_R$, which corresponds to the maximum load. For ideal elastic materials with $C_a = C_e$, the increase of up to $\tilde{G}_{R\,max}$ is relatively flat, but $\tilde{G}_R$ decreases with increasing displacement beyond the maximum load and decreasing load due to the term

$$PC_e\,\frac{dP}{da} = u_e\,\frac{dP}{da} \tag{5}$$

This may hold true for fine grained ceramics with vanishing microcracking. However, the $\tilde{G}_R$ curve of a ceramic with a measurable offset, shows a steep increase up to the pronounced maximum $\tilde{G}_{R\,max}$ close to the maximum load. This is well documented in the literature (5,12) (Fig. 2).

Micromechanically, crack resistance can be written as

$$\tilde{G}_R = \frac{2\gamma}{a_m} \; \psi \; I_m^2 + \psi \frac{d}{da}\left(\frac{2\gamma}{a_m}\right) \; \psi \; I_m^2 \tag{6}$$

where 2 γ, 2a_m and 2 ψ are the specific surface energy, average microcrack length, and the size of the process zone, respectively. I_m was introduced as the elastic interaction parameter in the following form

$$I_m = \sqrt{\frac{\beta E_m}{E - E_m}} \tag{7}$$

The parameter represents the deviation from linearity of brittle materials, and is a measure for the normalized strength. Fig. 3 shows the influence of the microcrack density β, and the reduced Young's modulus on this quantity. $\tilde{G}_R$ curve measurements by Osterstock and Tertel (4), show the influence of a reduction of the active microcrack nuclei due to thermomechanical loading (Fig. 4).

With measured values of eq. (6) and reduction of Young's modulus with SAM of 10% of alumina AF 997 (14), the table gives an estimate of a qualitative evaluation of $\tilde{G}_R$ of ceramics which allow the optimization of a specific microstructure. The microcrack density was assumed to be about 10%. This quantifies the parameter I_m as shown in Fig. 3.

CONCLUDING REMARKS

With the algorithm of this work it is proposed, that the $\tilde{G}_R$ curve behavior of some technical ceramics is due to residual stresses, which are introduced by the external work in the damage zone. They induce the offset. Within this context, the governing parameter is I_m (eq. (7)) as a function of β and E_m, including elastic interaction effects. These factors are not completely included in the formalism proposed by Budiansky et al. (15) in the derivation of Young's modulus. With this quantity, the parameter I_m follows as (6,10)

$$I_m = 3/4\sqrt{E_m/E} \tag{8}$$

The influence of Young's modulus on the $\tilde{G}_R$ curve, seems to be underestimated. Especially the influence of the residual stresses, including the offset, cannot be taken into account.
The influence of "mode II" microcracks on the $\tilde{G}_R$ curve seems to be the most questionable. Rough fracture surfaces indicate this fracture mode. It is proposed that high I_m values are a consequence of these features, which are in accordance with some fractografic observations. These measurements use the special decoration technique.

Crack initiation

$2a_m$	2γ	2ψ	E	G_0	S_m^2/E	S_m	l_m
µm	N/m	µm	GPa	N/m	MPa	MPa	
20	2	200	365	20	0,2	270	1

Stable crack growth as received

G_{rmax}			
N/m			
100	5,2	1370	5,1

Stable crack growth after thermal elastic damage

75	4,7	1300	4,7

Table showing measured and evaluated fracture mechanical parameters of alumina AF997.

REFERENCES

(1) Buresch, F.E., Euromech Collq., Paderborn 1989.

(2) Buresch, F.E., Frye K., Müller Th., Fracture Mechanics of Cerm. Vol. 5, 1983, 591.

(3) Buresch O., Buresch F.E., Hönle W., Schnering H.G. von, Microchim.Acta (Wien) 1987, I, 219

(4) Tertel A., 2. Studienarbeit, Clausthal Nov. 1987.
Osterstock F., Moussa R., Fortschr. Ber. DKG, Bd. 3, 1988, 3, 71.

(5) Babilon E., Bär K.K.O., Kleist G., Nickel H., Euro Ceramics, Vol. 3, 1989, 3.247.

(6) Buresch F.E., Materialpr. 29, 1987, 261–268.

(7) Mishima T., Nanayama Y., Hirose Y., Tanaka K., Advance in X-ray analysis, 30, 1987, 545–552.

(8) Buresch O., Müller M., Kromp K., Buresch F.E., ECF 7, Vol. 1, 1988, 546.

(9) Buresch I., personal communication.

(10) Buresch F.E., Adv. in Ceram., Vol. 12, 1984, 306.

(11) Claussen N., Cox R.I., Wallace J.S., Jour.Am.Cer.Soc., 1982, C 190.

(12) Buresch F.E., Materialpr. 32, 1990, 69.

(13) Nötzel G.W., critical remarks.

(14) Quinten A., Arnold W., Conf.Europ.Mat.Res.Soc.Jour.Mat.Sc.Eng. A 122, 1989, 15–19.

(15) Budiansky B.J., Hutchinson J.C., Lampropoulos J.C., Int.J.Solids Structures, 19, 1983, 337.

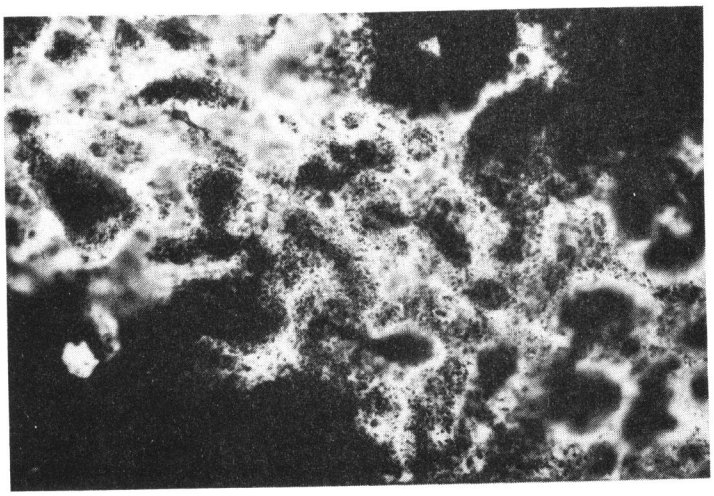

Figure 1. Microcracked damage zone surrounding a macrocrack of alumina due to thermal stresses (3,9)

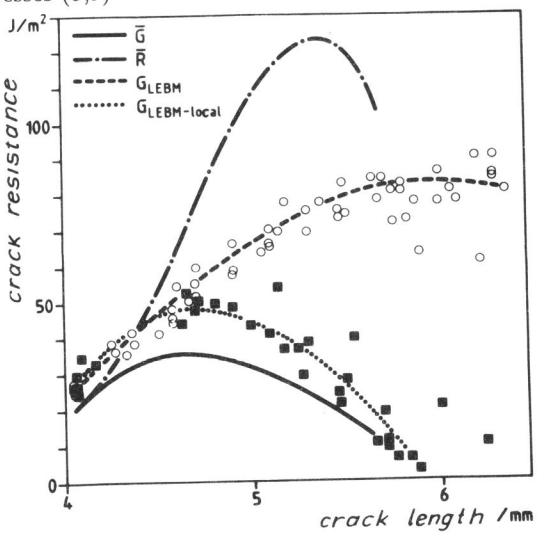

Figure 2. R curve of alumina AF 997, evaluated by (4) showing R using C_e and C_r, G_{LEMB} and $G_{LEMB-Local}$, only using C_a and C_e, respectively (4).

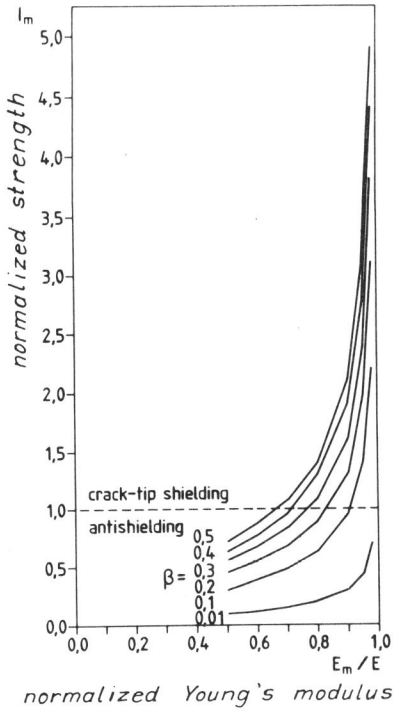

Figure 3. Normalized strength I_m, as a function of the microcrack density β and the related Young's modulus E_m/E (12).

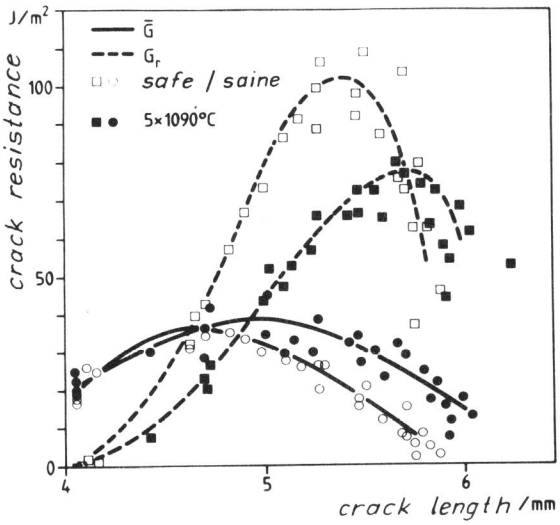

Figure 4. The same as Fig. 2, with values of thermomechanically predamaged materials (4).